**International Journal of Power Electronics and Drive Systems (IJPEDS)**
Vol. 15, No. 1, March 2024, pp. 222~238
ISSN: 2088-8694, DOI: 10.11591/ijpeds.v15.i1.pp222-238 

# Performance improvement of a standalone PV system using supercapacitors: modeling and energy management

**Mohamed Salah Hassan[1,2], Shimaa Hassan[1], Mohamed Reda Mahmoud Hassan[1], Abou-Hashema Mostafa El-Sayed[1], Masahito Shoyama[2], Gamal Mahmoud Dousoky[1,3]**
[1]Department of Electrical Engineering, Faculty of Engineering, Minia University, Minya, Egypt
[2]Department of Electrical Engineering, Faculty of Information Science and Electrical Engineering, Kyushu University, Fukuoka, Japan
[3]Department of Mechatronics Engineering, Nahda University, Beni-Suef, Egypt

**Article Info**

***Article history:***

Received May 6, 2023
Revised July 25, 2023
Accepted Aug 9, 2023

***Keywords:***

Energy management
PI controller
Pulsating load
Photovoltaic
Supercapacitor

**ABSTRACT**

Standalone photovoltaic (PV) systems are the most common and practical application in remote areas and communities far from the power grid. However, in the case of supplying a pulsating load with only a battery as a storage unit, their performance degraded. Therefore, hybrid electrical energy storage (HEES) systems represent a viable solution. This paper investigates the impact of utilizing a supercapacitor (SC) to work cooperatively with a battery storage unit to enhance the overall system behavior. Two scenarios of battery storage systems with/without SC are considered. A comprehensive modeling and sizing approach is established and presented in detail. Then, an energy management system (EMS) is proposed to enhance the HEES system's performance. A proportional-integral (PI)-based controller is designed and examined to control the power electronic converters and hence improve energy management. The HEES system operation is simulated and evaluated using MATLAB/Simulink to feed a pulsating load, where the drawn pulsated load current is composed of two components: one component is supplied by battery, and the other component is fed from SC. Finally, the performance of the two hybrid configurations is evaluated in terms of battery voltage and current fluctuations, transient response, and load voltage and current ripples. The obtained results demonstrate the effectiveness of introducing SCs into HEES system.



***Corresponding Author:***

Mohamed Saleh Hassan
Department of Electrical Engineering, Faculty of Engineering, Minia University
Damaris, Minya, 2431436, Egypt
Email: m.salah@mu.edu.eg

## NOMENCLATURE

| | | | |
|---|---|---|---|
| CESs | : Conventional energy sources | $d$ | : Helmholtz layer length (molecular radius) |
| EES | : Electrical energy storage | $R$ | : Ideal gas constant (in $J/K.mol$) |
| EMS | : Energy management system | $A_{PV}$ | : Ideality factor |
| EV | : Electric vehicles | $A_i$ | : Interfacial area between electrodes and electrolyte |
| FBC | : Filtration based controller | $C_{GC}$ | : Gouy-Chapman's capacitance |
| FLC | : Fuzzy logic controller | $P_{Load}$ | : Load demand power |
| HEES | : Hybrid electrical energy storage | $f_{LPF}$ | : Low-pass filter frequency |
| HEVs | : Hybrid electric vehicles | $c$ | : Molar concentration (mol$\cdot m^{-3}$) |
| LPF | : Low-pass filter | $N_e$ | : Number of electrode layers; |

MPP : Maximum power point
MPPT : Maximum power point tracking
PI : Proportional-integral
PSO : Particle swarm optimization
PV : Photovoltaic
RBC : Rule-based controller
RESs : Renewable energy sources
SC : Supercapacitor
$T$ : Ambient temperature (K)
$Q$ : Battery capacity (Ah)
$SoC_{int}$ : Battery initial state of charge
$R_{int}$ : Battery internal resistance
$SoC_{bat}$ : Battery state of charge
$K$ : Boltzmann's constant
$Q_c$ : Cell electric charge
$i_{sc}$ : Current of the SC module
$V_{Load}$ : DC load bus voltage
$D_1$ : Duty cycle of Q1 in the bi-directional buck-boost converter
$E_{go}$ : Silicon bandgap (~1.1eV)
$q$ : Electron charge
$A$ : Exponential zone amplitude (V)
$B$ : Exponential zone time constant inverse ($\text{Ah}^{-1}$)
$F$ : Faraday constant (in $C/mol$)
$C_H$ : Helmholtz's capacitance
$T$ : Operating temperature (K)
$V_{SC}$ : Output voltage of supercapacitor
$\varepsilon_0$ : Permittivity of free space
$\varepsilon$ : Permittivity of the electrolyte material
$I_{Ph}$ : Photocurrent source
$K$ : Polarization voltage (V)
$V_{ref}$ : Preset reference bus voltage
$P_{PV}$ : PV output power
$I_{Bat}^*$ : Reference battery current
$I_{SC}^*$ : Reference SC current
$I_{ref}^*$ : Reference total current
$T_{ref}$ : Reference temperature (298 K)
$I_{rs}$ : Reverse saturation current of module
$I_0$ : Saturation current
$R_S$ : Series resistor
$K_{SC}$ : Short circuit current temperature coefficient
$R_{Sh}$ : Shunt resistor
$D_2$ : Duty cycle of Q2 in the bi-directional buck-boost converter
$\lambda$ : Solar irradiance
$R_{SC}$ : Supercapacitor internal resistance (in Ω)
$E$ : The controlled voltage source in battery model
$C_T$ : Total capacitance of a SC cell
$V_{Bat\ or}$: Voltage across the storage element

## 1. INTRODUCTION

Due to expanding environmental concerns regarding excessive energy consumption, weather fluctuations, stratospheric ozone depletion, and the dependency of traditional energy sources on fossil fuels that cannot be maintained over the long term, it is becoming increasingly essential to transition from finite, non-renewable sources like fossil fuels to more sustainable and environmentally friendly alternatives. Owing to the advantages of such renewable energy sources (RESs) over conventional energy sources (CESs), including being clean, affordable, and limitless, many types of RESs, such as solar energy, wind energy, biomass energy, and hydropower have gained popularity in countries all over the world [1]. Using photovoltaic (PV) cells to generate electricity has many benefits, including being silent, cheap to maintain and run, and it can be used as an integral part of the design process for new structures [2].

Standalone PV systems are the most common and practical application, especially in remote areas and communities far from the power grid, but their reliability is influenced by atmospheric conditions, such as temperature and solar radiation [3]. Electrical energy storage (EES) can help address these challenges by fulfilling the demand specifications in the absence or deficiency of PV power generation. EESs have many characteristics and features, and no one EES technology can meet all the desired requirements of a given application, including power densities, energy densities, charge/discharge rates, and load profiles, including pulsating loads (loads that vary rapidly over time). Consequently, hybrid electrical energy storage (HEES) systems represent a viable solution [4], which might include a high-power, low-energy density technology for handling the peaks in demand, along with a low-power, high-energy density technology for handling the baseline load.

The simplest configuration of EES in a standalone PV system is illustrated in Figure 1 which comprises lead-acid batteries. Such an EES has a poor reliability nature, which cannot confidently fulfill the desired load profile in terms of power and charge/discharge rates [5]. Certain loads, such as motors, refrigerators, and air conditioners, require an initial surge current, which can be several times greater than their regular operating current [6]. However, these large current demands are only required for short periods, usually, a few seconds to a minute, and then the current demand drops to a much lower level. One solution to address this issue is to use an inverter with a surge rating to provide a burst of power that is capable of handling the high starting current of the load. Another option is to use a capacitor bank in conjunction with a battery storage system since sizing a battery storage unit capable of providing this high current demand is costly and bulky. Moreover, some battery storage units may need to be replaced every three to five years, while others may last much longer with proper maintenance and care.

Supercapacitors, also known as ultracapacitors, are energy storage devices capable of storing much more energy than traditional capacitors but less energy than batteries. They have a high power density, which means they can deliver a high surge of power rapidly, and are also able to charge and discharge very quickly. Additionally, because SCs have a very high cycle life (the number of times they can be charged and discharged), they can provide a reliable and long-lasting solution for addressing high starting current demands. In the context of addressing high starting current needs, a SC can be used to provide the initial surge of energy needed by the load. When the load is switched on, the SC can discharge quickly to deliver the high current required for starting. Once the load has started, the battery storage unit can take over to supply the continuous power needed for running the load. Therefore, short-term power bursts and battery power supply stabilization are significant contributors to the growth of SCs.

Many studies have shown that the battery-SC HEES systems can make the battery last longer by reducing the stress caused by charging and discharging [7], [8]. However, the majority of these battery-SC HEES systems require an entire remodeling of the ESS, which may not be financially viable particularly for remote applications. In this context, [9] proposed a smart hybrid energy storage plug-in unit with the aim of extending the operational lifespan of lead-acid batteries in standalone PV-battery power systems by reducing the effects of current changes and surge currents that shorten the battery's life. Ma *et al.* [10] explored a passively connected HEES system for renewable energy distribution in off-grid locations. However, the unpredictability of the terminal voltage of SC banks and the lack of a clearly defined current share between the battery and SC make the active connected HEES a necessity, in which the power converter is embedded.

Topology and complexity of existing HEES systems and associated EMSs vary widely and are typically based on the specific application. When it comes to extending the life of Lead-acid batteries in rural standalone PV home energy systems, Jing *et al.* [11] provided a thorough analysis of the current state of the art. Parameter and state estimation, aging mechanism and lifespan prediction, and energy optimization control have also been discussed in [12] has also delved into research area including the estimation of parameters and states, the examination of aging mechanisms along with forecasting lifespans,, in which a thorough assessment of critical concerns in the control and management of the HEES systems has been provided. Zhang *et al.* [13] suggested an EMS for electric vehicles (EV) battery and SC HEES that operated in real time. The technique incorporated a wavelet transform, neural network, and fuzzy logic controller (FLC) to address both the peak and fluctuating power requirements of a battery. Therefore, a 44.22% increase in the amount of regenerative braking energy recovered has been achieved compared to the standard filtration-based control technique, and the battery life cost has been decreased by 18%.

The result in [14], a comparison has been carried out between a standalone PV system with a battery-SC HEES facility and a traditional PV system with only batteries for a rural household. Two control techniques have been suggested in this study: rule-based controller (RBC) and filtration-based controller (FBC). The words in [15], a real-time EMS for a semi-active HEES system based on a combination of filtering and FLC has been theoretically developed and experimentally verified. The primary benefit of this control method is its ability to obviously lower the battery's peak current while guaranteeing the SC voltage stays within a predetermined range. Unlike traditional control schemes, which only make use of FBC or FLC, Chong *et al.* [16] developed an optimal control approach for a standalone PV system with HEES that uses both a low-pass filter and FLC. The particle swarm optimization (PSO) algorithm was utilized to tune membership function so that battery peak current reduction could be optimized.

Due to non-monotonic energy consumption and rapid variations throughout the battery discharging process which severely harmed the electrochemical process of the battery, present battery technologies do not satisfy the energy demands of EV power consumption. Similar to systems in remote locations, couplings between the batteries and SCs in the form of HEES appear to be the optimal method for extending the battery life in EVs. Consistent, efficient, and secure operation of HEES systems requires the development and application of a suitable realistic control technique. In this context, Kouchachvili *et al.* [17] proposed combining batteries with SCs, which give higher rate capability and improved cyclability by rapidly supplying more energy when the battery runs low. After that, the battery pack provides a constant supply of energy. The HEES has received a lot of attention because of its potential use in plug-in hybrid electric vehicles (HEVs). However, relatively few analyses of its architecture and EMSs have been conducted. Accordingly, an interesting survey on the structures and the EMSs of HEES systems has been discussed in [18]. By regulating the battery charge/discharge rate effectively, the battery service life can be extended, and the system lifespan cycle cost can be decreased. In this review, the optimization algorithms applied for the HEES systems in terms of energy management have been classified and emphasized. Furthermore, Lemian and Bode [19] presented a comprehensive overview of recent advancements in energy storage, power converters, approaches for energy management, and control algorithms employed in vehicles.

In summary, the gap in this study lies in the performance degradation of standalone PV systems when supplying pulsating loads using only battery storage units. While HEES systems have been proposed as a

solution, there is a lack of comprehensive investigation on the specific impact of integrating SCs into such systems. This research aims to fill this gap by exploring the cooperative operation of SCs and battery storage units to enhance the overall performance of the standalone PV system when subjected to pulsating loads. Therefore, the salient contributions of this paper can be outlined as follows:
- A detailed model of a hybrid PV system including HEES is introduced.
- The theoretical analysis of the proposed EMS applied to the hybrid system is demonstrated.
- The performance analysis of the hybrid system under different operating conditions such as solar radiation change, and different loads is investigated.
- The evaluation of the two hybrid systems under pulsating load conditions, where the drawn current is supplied jointly by the battery and the supercapacitor, is a unique aspect of our research.

This paper comprises six main sections. Section 2 delves into the modeling aspects of the hybrid energy storage system (EES), which encompass the modeling of the PV array, the battery storage unit, the supercapacitor (SC), and the associated DC/DC converters. Moving on to section 3, the specifications for system sizing have been discussed. In section 4, the proposed energy management system (EMS) control strategy has been introduced. Section 5 is dedicated to showcasing the test results of the hybrid system under two different scenarios: one without the supercapacitor and the other incorporating the supercapacitor. Finally, Section 6 provides an overview of the key conclusions and findings derived from the present research.

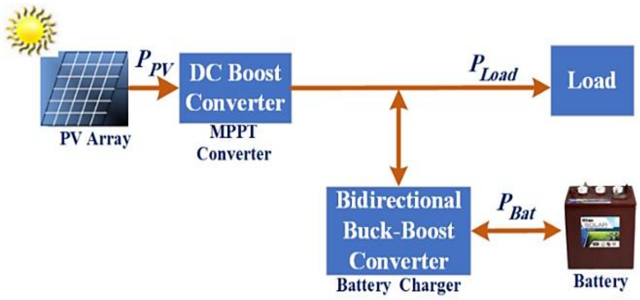


Figure 1. A typical PV-battery standalone system

## 2. OVERALL SYSTEM MODILING

To achieve optimal performance in standalone PV systems using SCs, it is necessary to develop accurate models and effective energy management strategies. This involves understanding the behavior of the system under different operating conditions and controlling the flow of energy between the PV panels, SCs, batteries, and load. In this context, the proposed hybrid PV system mainly comprises PV, battery, and SC as illustrated in Figure 2. The EES system consists of a combination of SC and batteries. Both the SCs and batteries are connected to the DC bus through bi-directional buck-boost converters. The models of system units are introduced in the following subsections:

### 2.1. Photovoltaic model

The fundamental component of the energy conversion system under investigation is the solar cell, which serves as its core element. Solar cells are essentially large semiconductor diodes characterized by an interface between P- and N-doped silicon. Figure 3 illustrates the equivalent circuit for a solar cell, comprising a current source carrying a photocurrent ($I_{Ph}$), a diode that symbolizes the P-N junction in the PV cycle, a shunt resistor ($R_{Sh}$) responsible for managing the leakage current, and a series resistor ($R_S$) accounting for internal resistance to current flow. The photocurrent of the module can be mathematically expressed, as demonstrated in [1], [20]:

$$I_{ph} = \frac{\lambda}{1000}\left(I_{SCr} + K_{SC}(T - 298)\right) \quad (1)$$

where $\lambda$ is solar irradiance, $I_{SCr}$ is the PV cell short circuit current at 25 °C and 1000 W/m$^2$, $K_{SC}$ is the short circuit current temperature coefficient and $T$ is the ambient temperature (K). The current-voltage characteristic of a PV cell is given as (2),

$$I_{PV} = I_{ph} - I_0\left[exp\left(\frac{q(V_{PV}+I_{PV}R_S)}{A_{PV}KT} - 1\right) - \frac{V_{PV}+I_{PV}R_S}{R_{Sh}}\right] \quad (2)$$

where $I_0$ refers to the saturation current, $q$ represents the electron charge, $A_{PV}$ is the ideality factor, and $K$ is the Boltzman's constant. In order to simplify the analysis, the expression of current-voltage characteristics can be rewritten as (3).

$$I_{PV} = I_{ph} - I_0\, exp\left(\frac{q(V_{PV}+I_{PV}R_S)}{AKT} - 1\right) \tag{3}$$

The saturation current can be expressed as (4),

$$I_0 = I_{rs}\left(\frac{T}{T_{ref}}\right)^3 exp\left[\frac{qE_{go}}{AK}\left(\frac{1}{T_{ref}} - \frac{1}{T}\right)\right] \tag{4}$$

where $T_{ref}$ is the reference temperature (298 K), $I_{rs}$ is reverse saturation current of module, and $E_{go}$ is the silicon bandgap ($\sim 1.1eV$). Several number of PV modules are connected in series and parallel to form a PV array in order to generate the desired voltage, current, and hence the power rating. Accordingly, the PV array output current can be determined from as (5).

$$I_{PV} = N_P I_{ph} - N_P I_0\left[exp\left(\frac{q(N_P V_{PV}+I_{PV}R_S N_S)}{N_S N_P AKT}\right) - 1\right] \tag{5}$$

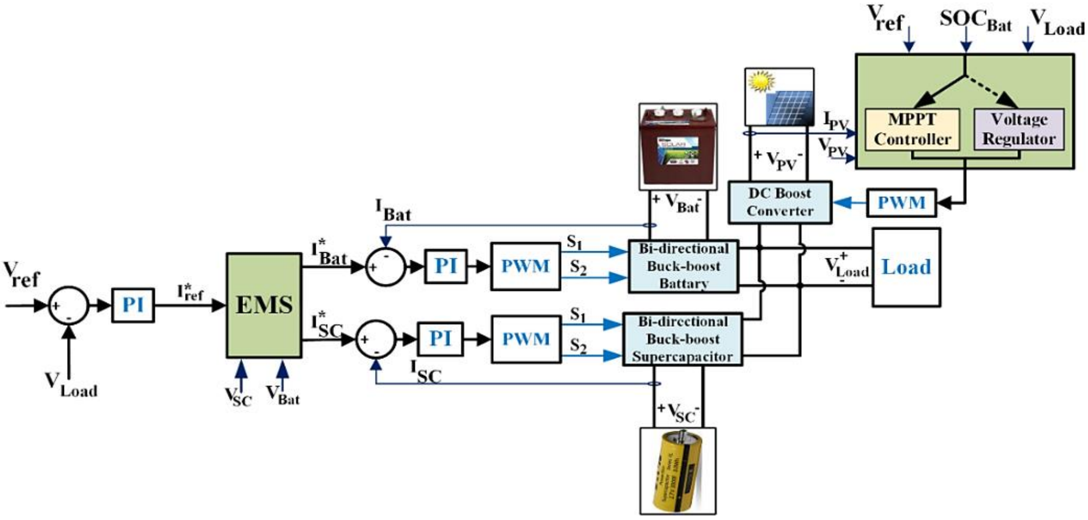


Figure 2. Block diagram of the proposed hybrid PV, battery, and SC system

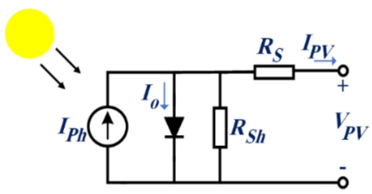


Figure 3. The PV model equivalent circuit

### 2.2. Battery model

Lead acid batteries are widely employed as energy storage devices in photovoltaic (PV) systems. A common model for the battery involves representing it as a straightforward controlled voltage source connected in series with an internal resistance (denoted as $R_{int}$) as depicted in Figure 4 [2], [21]. The voltage at the battery terminals is characterized as (6),

$$V_{Bat} = E - R_{int} \times I_{bat} \tag{6}$$

where $E$ is the controlled voltage source which is given by (7) [22]:

$$E = E_0 - K\frac{Q}{Q-\int i_{bat}dt} + Ae^{-B\int i_{bat}dt} \tag{7}$$

where $E_0$ is the battery constant voltage, $K$ is the polarization voltage (V), $Q$ is the battery capacity (Ah), $A$ is the exponential zone amplitude (V), and $B$ is the exponential zonetime constant inverse (Ah$^{-1}$). The battery state of charge ($SoC_{bat}$) is given by (8),

$$SoC_{bat} = SoC_{int} - \frac{1}{Q}\int idt \tag{8}$$

where $SoC_{int}$ is the initial state of charge.

### 2.3. Supercapacitor model

Numerous models have been developed to represent the behavior of a SCs in [23]. From which, Figure 5 shows the stern model of SCs. This model is practical for simulation applications and for demonstrating the nonlinear capacitance nature, which combines both Helmholtz's capacitance ($C_H$) and Gouy-Chapman's capacitance ($C_{GC}$). The total capacitance of a SC cell is described as (9) [24], [25],

$$C_T = \frac{N_p}{N_s}\left[\frac{1}{C_H} + \frac{1}{C_{GC}}\right]^{-1} \tag{9}$$

where $N_p$is the number of parallel SCs and $N_s$ is the number of series SC cells. The Helmholtz's capacitance ($C_H$) and Gouy-Chapman's capacitance ($C_{GC}$) are expressed as (10) and (11),

$$C_H = \frac{N_e\varepsilon\varepsilon_0 A_i}{d} \tag{10}$$

$$C_{GC} = \frac{FQ_c}{2N_eRT}sinh\left(\frac{Q_c}{N_e{}^2A_i\sqrt{8RT\varepsilon\varepsilon_0 c}}\right) \tag{11}$$

where $N_e$ representing the number of electrode layers; $\varepsilon$ denoting the permittivity of the electrolyte material, $\varepsilon_0$ indicating the permittivity of free space, $A_i$ representing the interfacial area between electrodes and electrolyte, $d$ signifying the Helmholtz layer length (molecular radius), $Q_c$ depicting the cell electric charge, $c$ denoting the molar concentration (in mol$\cdot m^{-3}$), $T$ representing the operating temperature (K), $R$ representing ideal gas constant (in $J/K.mol$), and $F$ indicating the Faraday constant (in $C/mol$). The output voltage of the SC is expressed as shown in (12), while accounting for the internal resistance losses.

$$V_{SC} = \frac{\int i_{SC}dt}{C_T} - R_{SC}i_{SC} \tag{12}$$

where $R_{SC}$ is the internal resistance (in Ω) and $i_{sc}$ is current of the SC module.

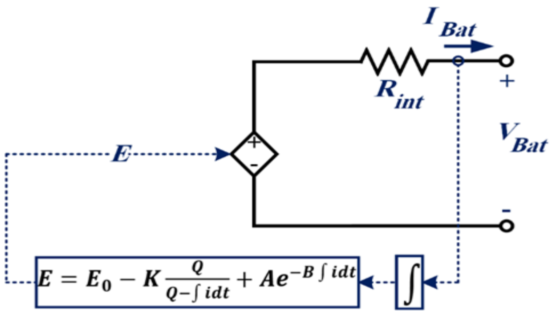


Figure 4. The lead acid battery model

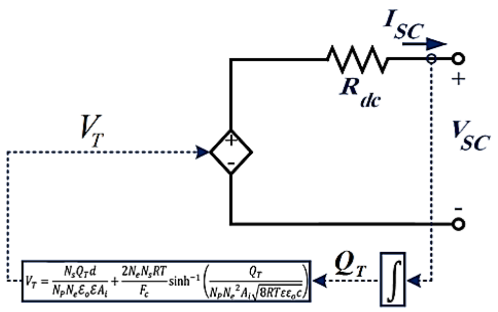


Figure 5. Schematic diagram of the SC stern model

### 2.4. Modeling of DC/DC converters

The PV array, battery, and supercapacitor systems are linked to the DC bus using DC/DC converters, providing comprehensive control over both the PV array and the energy storage systems (EES) components.

The system incorporates two distinct types of DC/DC converters: the DC/DC boost converter and the bi-directional buck-boost converter.

### 2.4.1. Boost converter model

The power stage of the boost converter is used to implement maximum power point (MPP) tracking (MPPT). Its equivalent circuit is shown in Figure 6. It is composed of the single pole double throw switch (transistor and diode combination), the smoothing inductance ($L_{Boost}$), and the output smoothing capacitor ($C$), which is attached between the PV array and the DC bus.

### 2.4.2. Bidirectional buck boost converter model

The battery and SC storage units are connected to the DC load bus through the bi-directional buck-boost. This allows voltage control of the DC bus load as well as control of the battery and SC currents simultaneously [26]. The power stage of the converter is described in Figure 7. It consists of two switches $Q_1$ and $Q_2$, smoothing inductance $L$ and output smoothing capacitance $C$. In case of buck converter mode, $Q_2$ is always OFF and current flows from the DC bus to the battery and/or the SC. By controlling the duty ratio $D_1$ of the switch $Q_1$, the converter decreases the DC load bus voltage ($V_{Load}$) to charge the battery and/or supercapacitor. The voltage across the storage element can be expressed as (13).

$$V_{Bat\ or\ SC} = D_1 V_{Load} \tag{13}$$

Switch $Q_1$ is always OFF in boost mode and current flows from the battery and/or the SC to the DC load bus. By controlling the duty ratio $D_2$ of the switch $Q_2$, the converter can increase the battery and/or SC voltages to the DC load bus voltage, which can be expressed as (14).

$$V_{Load} = \frac{V_{Bat\ or\ SC}}{1-D_2} \tag{14}$$

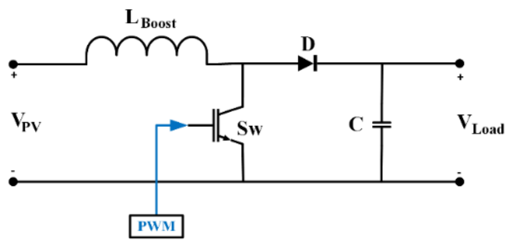


Figure 6. Equivalent circuit of the DC-DC boost converter

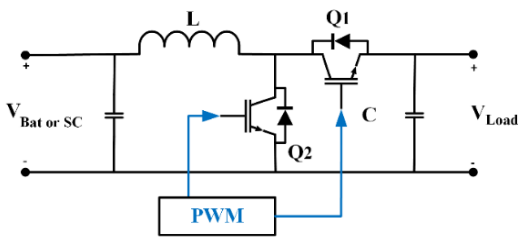


Figure 7. The bi-directional buck-boost converter power stage

## 3. SYSTEM SIZING

It is paramount to accurately size the battery storage unit to ensure it is able to provide the continuous power required by the load in normal conditions without surge current. On the other hand, the size and capacity of the SC required depend on the specific load and the duration of the surge current. A representative short time window of the utilized load profile is illustrated in Figure 8, which consists of a 1350 W continuous load in addition to a 540 W pulsating load during the intervals (0.4 to 0.6 s) and (1.4 to 1.6 s). Such load demands represent a residential load attached to a farm in a remote agricultural area; similar to those loads addressed in reference [27], in which the pulsating load in this paper can be assumed as an automatic washing machine. In order to supply this load, the PV array, storage battery, SC bank, and DC-DC converters are designed, and accordingly sized as illustrated in Tables 1, 2, 3, and 4.

Table 1. The PV array sizing specifications

| PV array power | PV module power | PV module MPP voltage | PV module MPP current | No. of series modules | No. of parallel branches |
|---|---|---|---|---|---|
| 2.7 kW | 270 W | 31.4 V | 8.76 A | 2 | 5 |

Table 2. The sizing specifications of battery storage units

| Battery voltage | Battery capacity | Required battery capacity | No. of series batteries | No. of parallel branches |
|---|---|---|---|---|
| 12 V | 150 Ah | 1200 Ah | 2 | 4 |

Table 3. The SC bank sizing specifications

| SC voltage | SC capacitance | Required SC capacitance | No. of series SCs | No. of parallel branches |
|---|---|---|---|---|
| 2.7 V | 3000 F | 250 F | 12 | 1 |

Table 4. The DC/DC converters parameters

| | Bi-directional battery converter | Bi-directional SC converter | MPPT boost converter |
|---|---|---|---|
| Inductance | 0.3 mH | 0.2 mH | 0.35 mH |
| Switching frequency | 16 kHz | 16 kHz | 16 kHz |
| Low voltage | 24 V | 32 V | PV output voltage |
| High voltage | 50 V | 50 V | 50 V |
| Low voltage side capacitor | 16 μF | 22 μF | 470 μF |
| DC load bus capacitor | | 470 μF | |

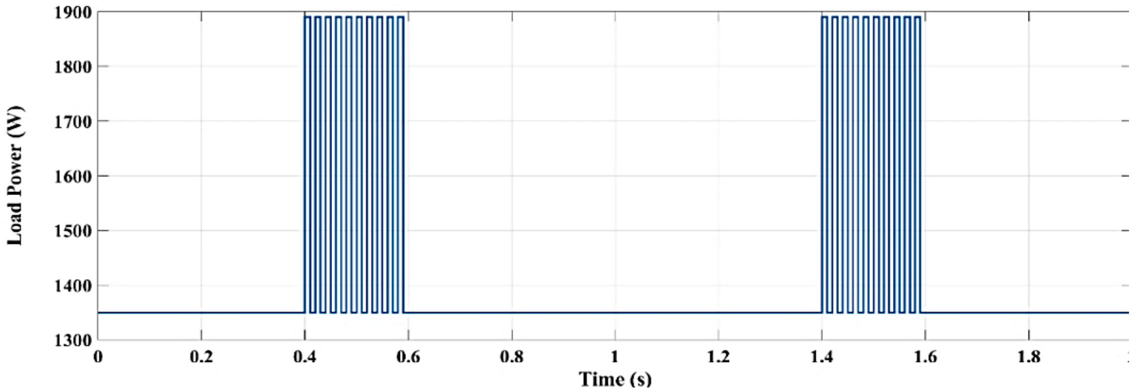


Figure 8. A representative short time window of the utilized load profile

## 4. ENERGY MANAGMANT SYSTEM

Implementing an energy management system (EMS) is crucial to enhancing the performance of a standalone PV system that utilizes a HEES system with batteries and SCs. The HEES system can store excess energy generated by the PV system during peak sunlight hours and provide it during periods of low sunlight, reducing reliance on non-renewable energy sources and improving energy efficiency. To optimize the performance of HEES in standalone PV systems, an EMS is typically employed. Such a system involves monitoring and controlling the energy flow between PV panels, batteries and SCs to maximize their efficiency and lifespan while meeting the energy demands of the system. This involves developing algorithms that balance the energy stored in each device, avoid battery deep discharge, minimize the battery dynamic stress level, and preserve a constant DC load voltage. These factors can impact the efficiency and lifespan of the energy storage components and must be considered in the design and operation of the system.

The main idea of the EMS is that the battery unit supplies low frequency power components while the SC provides high frequency power components in short period of time. In this context, the load bus voltage ($V_{Load}$) is measured and compared with the preset reference bus voltage ($V_{ref}$). The result of comparison is passed through the PI regulator in order to compensate the DC bus voltage by providing the reference total current ($I_{ref}^{*}$) that is required to be supplied by the hybrid energy sources. After that, this total current is decoupled into two components, the average component and the pulsating component, using the low-pass filter (LPF) as illustrated in Figure 9 where ($f_{LPF}$) refers to the LPF functionality. The proposed EMS algorithm provides two current components: the reference battery current ($I_{Bat}^{*}$) that is obtained from average component the total current, whereas the reference SC current ($I_{SC}^{*}$) that is estimated by the pulsating component of the total current.

Accordingly, and based on the flowchart shown in Figure 10, the implementation and operation of the proposed EMS strategy for DC bus voltage regulation can be described as follows. The SCs start to charge when PV output power is higher than load demand power ($P_{PV} > P_{Load}$), and batteries cannot preserve such excessive power in short periods of time. On the other hand, the SCs tend to discharge in cases of insufficient available PV power to fulfill the load demand ($P_{PV} < P_{Load}$), in which the batteries cannot deliver the extra power required to the load. On the other hand, the SCs can respond directly to the required load demand by providing or absorbing peaks currents.

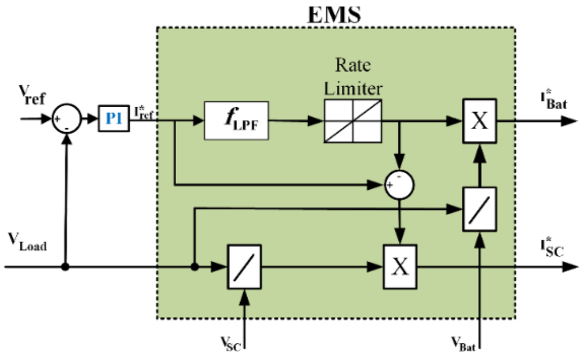


Figure 9. Schematic block diagram of the EMS strategy implementation

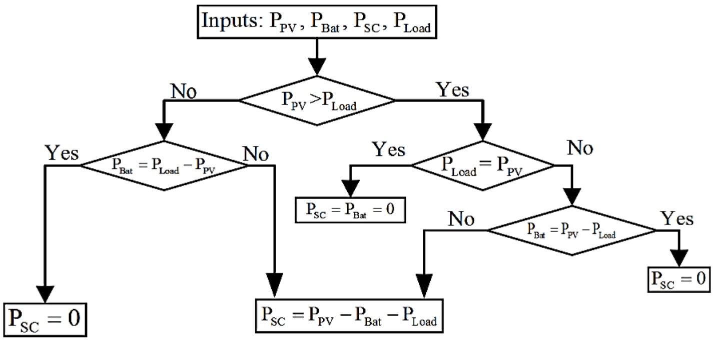


Figure 10. The EMS control strategy of the DC bus control in terms of power

The following considerations are taken into account during the EMS design:

a) The main task of the battery and the associated bi-directional converter is to regulate the load DC bus voltage and supply the load demand in case of PV power deficit.
b) The system is designed to increase the surplus PV power by charging both battery and SC until they reach their maximum affordable SoC.
c) If the battery is out of service due to low SoC, the PV boost converter operates as voltage regulator to compensate the absence of battery and achieve the job addressed in (I).
d) If the available PV power is higher than the load demand, the PV converter operates as a MPPT, and accordingly, both of battery and SC are allowed to charge until the maximum permissible SoC is reached.
e) The SC converter control's priority is to feed the pulsating component of the load demand to release the dynamic stress burden on the battery, which increase its lifespan.

These considerations suggest that the EMS is designed to optimize the use of available resources, regulate the system voltage and current, and protect the battery and SC from overcharging and over discharging. By taking into account the load demand, PV power availability, and battery state of charge, the EMS can ensure reliable and efficient operation of the system.

## 5. RESULTS AND DISCUSSION

In order to investigate the overall system performance with the proposed EMS strategy, the system model is simulated using the MATLAB/Simulink software packages. The parameters of the PV array, battery, and SC are addressed in Tables 5, 6, and 7, respectively. The load profile, shown in Figure 8, is assumed to have a base demand describing a residential resistive load in addition to a pulsating load representing an automatic washing machine. Solar radiation is a vital parameter in the operation of PV systems, and its variation over the course of a day is a key factor that affects the performance of a standalone PV system. In this paper, the solar radiation, shown in Figure 11, is assumed to be changed instantly at the 1 s from 1000 W/m$^2$ (i.e., sunny day) to 500 W/m$^2$ (i.e., cloudy day), which can be considered as the worst case to figure out the impact of the proposed control strategy. Therefore, the system is evaluated under variations of load profile illustrated in Figure 8, as well as solar radiation shown in Figure 11. The following results are presented in such a way to show the impact of using SC alongside the proposed EMS strategy on the described standalone PV system (PV-battery system). These results can be discussed as follows:

Table 5. PV array parameters

| | Parameter | Value | Unit |
|---|---|---|---|
| PV Array | PV array power | 2.7 | kW |
| | No. of series modules | 2 | |
| | No. of parallel branches | 5 | |
| PV module parameters | Peak Power $P_{MAX}$ | 275 | W |
| | Maximum Power Voltage | 31.4 | V |
| | Maximum Power Current | 8.76 | A |
| | Open Circuit Voltage | 38.4 | V |
| | Short Circuit Current | 9.24 | A |
| | $R_s$ | 0.35 | Ω |
| | $R_{sh}$ | 1491.71 | Ω |
| | Nominal operating cell temperature (NOCT) | 44 | °C |
| | Temperature coefficient of $P_{MAX}$ | -0.39 | %/K |
| | Temperature coefficient of $V_{OC}$ | -0.29 | %/K |
| | Temperature coefficient of $I_{SC}$ | 0.05 | %/K |

Table 6. Battery parameters

| | Parameter | Value | Unit |
|---|---|---|---|
| Battery Array | Required battery capacity | 1200 | Ah |
| | No. of series Batteries | 2 | |
| | No. of parallel branches | 4 | |
| Battery parameters | Battery constant voltage ($E_0$) | 12.6463 | V |
| | Battery polarization constant ($K$) | 0.33 | V |
| | Battery capacity ($Q$) | 150 | Ah |
| | Battery exponential zone amplitude ($A$) | 0.66 | V |
| | Battery exponential zone time constant inverse ($B$) | 2884.61 | $(Ah)^{-1}$ |
| | Internal resistance of the battery ($R_{int}$) | 0.1 | Ω |

Table 7. Supercapacitor parameters

| | Parameter | Value | Unit |
|---|---|---|---|
| Supercapacitor array | Required supercapacitor capacitance | 250 | F |
| | No. of series supercapacitor | 12 | |
| | No. of parallel branches | 1 | |
| Supercapacitor parameters | Capacitance ($C$) | 3000 | F |
| | Rated Voltage | 2.7 | V |
| | $R_{SC}$ | 2.1 | mΩ |
| | $N_s$ | 1 | |
| | $N_p$ | 1 | |
| | $N_e$ | 2 | |
| | $d$ | 1.0115 | nm |

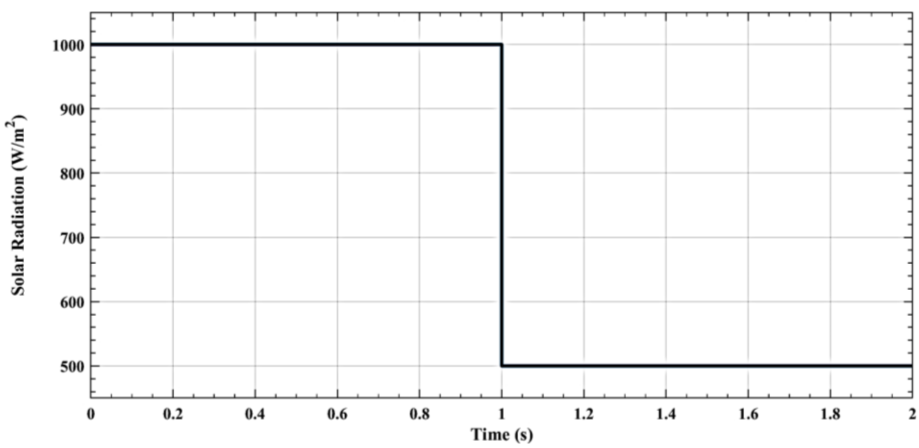


Figure 11. Assumed variation of solar radiation

The use of SCs with the proposed EMS control strategy led to an improved load voltage waveform, described in Figure 12, and a load current waveform shown in Figure 13. This improvement is observed in fast dynamic response and low ripple content in both high- and low-solar radiation levels. This can be confirmed at the zoomed starting instants of Figures 12 and 13, in which load voltage and load current with the SCs included reached the steady state value faster. Meanwhile, the voltage and current ripples are comparable with and without incorporating the SCs in the first period of applying the pulsating load in high-solar radiation (from 0.4 s to 0.6 s) compared to their counter values in the second period of supplying the pulsating load in low-solar radiation (from 1.4 s to 1.6 s). This is because during the period of 0.4 s to 0.6 s, the generated power from the PV system is higher than the required load power, in which the battery is charging.

Conversely, during periods of limited solar radiation, the power generated by the PV system falls short of the necessary load power. Consequently, this imbalance results in notable spikes in both load voltage and current ripples, primarily caused by the discharge state of the battery. Noteworthy, such undesirable surges for battery lifespan have obviously been filtered out during the period of pulsating load due to the presence of SCs that feature a rapid response to compensate for the surplus energy in the load. The robustness of the proposed EMS control strategy for the HEES is evaluated at the instant of changing the solar radiation at 1 s. The overshoot load voltage and load current responses have been considerably reduced in case of utilizing SC with a battery as a HEES system.

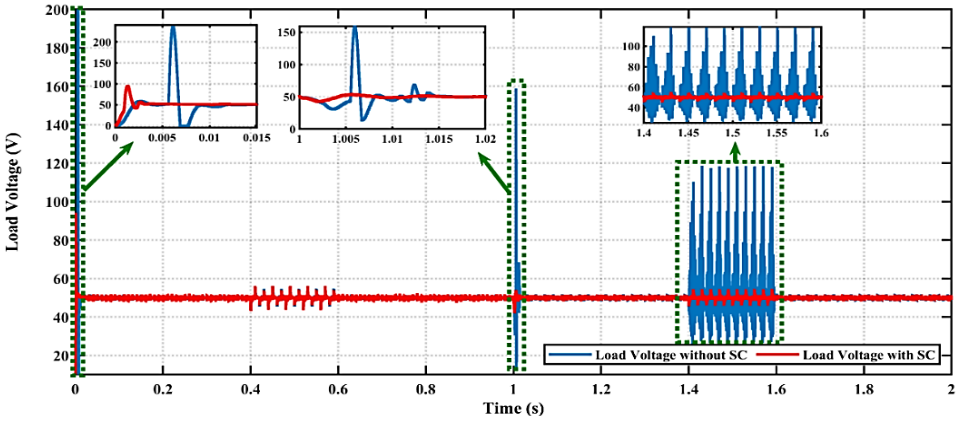


Figure 12. Simulated load bus voltage waveforms

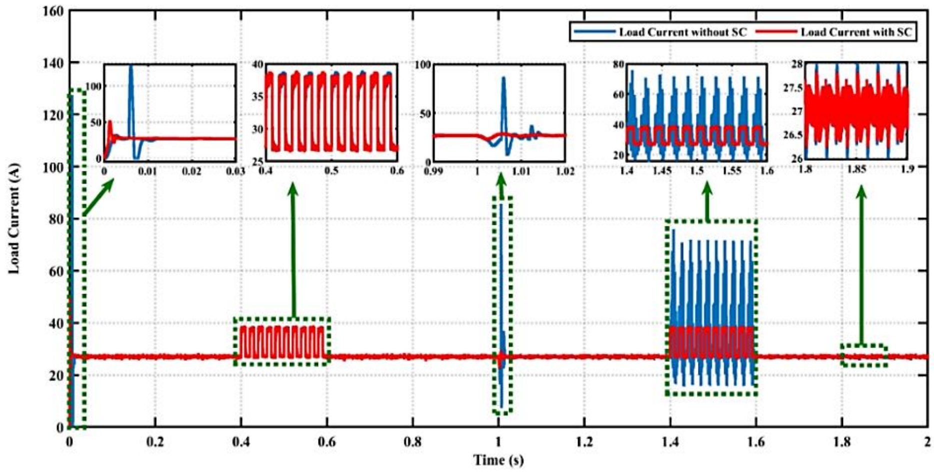


Figure 13. Simulated load current waveforms

Figures 14, 15, and 16 demonstrate the impact of using SC alongside the EMS strategy on the MPPT of the PV system. It has been observed that the use of SCs with the EMS strategy improved the MPPT response, at both high- and low-solar radiation levels. Furthermore, both the PV voltage and current fluctuations have been extensively reduced in case of pulsating loads, as illustrated in Figures 14 and 15. Moreover, the tracking behavior of the MPPT is increased under the pulsating load with low-solar radiation in case of including the SC along with the proposed EMS compared to the system with battery storage only that has been affected by the load voltage variation. The unacceptable voltage and current performance of the battery during the low-solar radiation and pulsating load periods negatively affected the generated output power from the PV system, as shown in Figure 16, in which the PV system with battery storage only exhibits a reduction in its generated power compared to the SC case, as illustrated in Figure 16. The improved PV system performance is due to the SC integration's ability to absorb the high pulsating load demand.

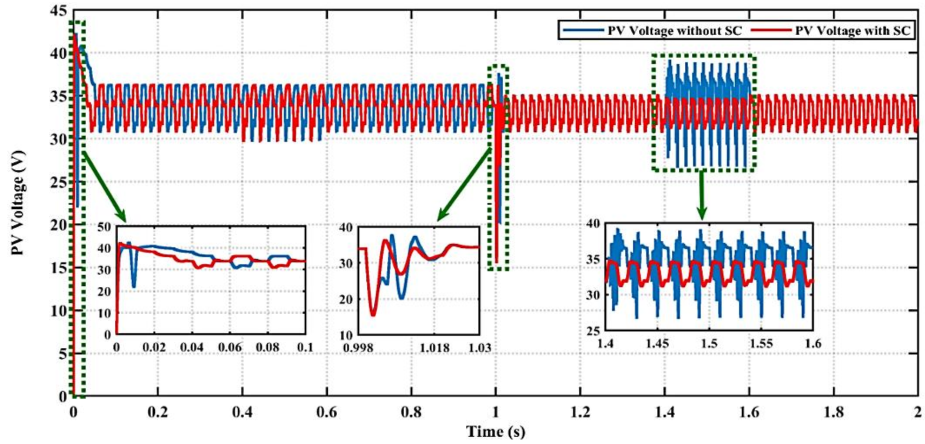


Figure 14. Simulated PV voltage waveforms

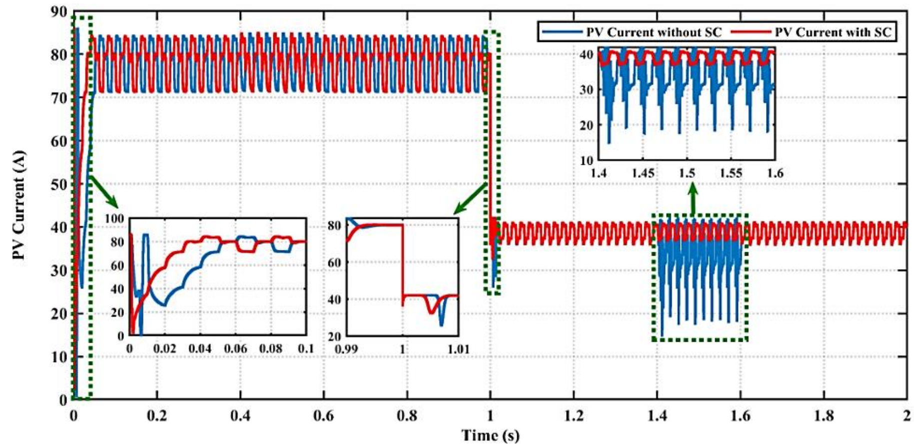


Figure 15. Simulated PV current waveforms

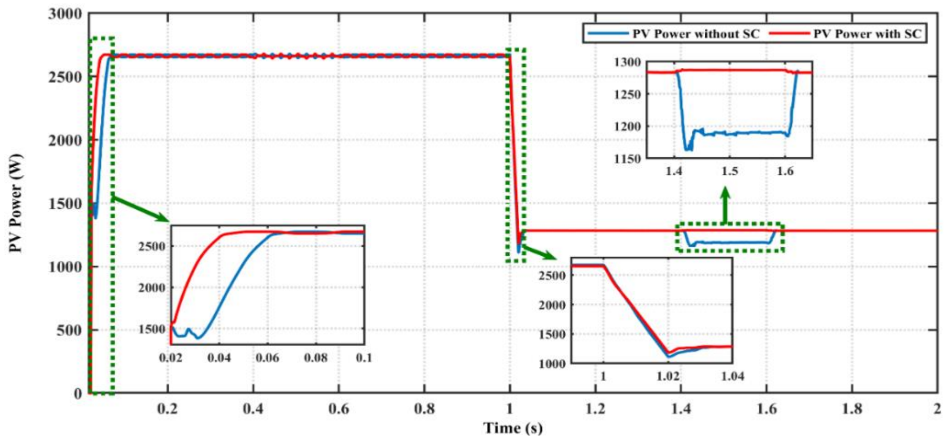


Figure 16. Simulated PV power waveforms

Figures 17 to 20 show the effect of using the HEES system, including the SC and the proposed EMS control strategy, on the battery's performance and operation. During startup, as can be seen from Figures 17, 18 and 19, the battery storage unit exhibits a more stressed operation than the HEES system due to the required load demand just before the MPPT system enters its operational state. Such a starting state requires the battery to supply higher current, as observed in Figure 18, which leads to undervoltage of the battery, as shown in Figure 17. This could be worsened in case of feeding a load with high starting current from the battery storage unit. In addition, the short-term variation of battery current and voltage observed in the starting instant could affect the battery's operation and degrade its performance.

Moreover, the superiority of utilizing the SCs is obviously observed in battery performance during the period of applying the pulsating load (from 0.4 s to 0.6 s and from 1.4 s to 1.6 s) either in high- or low-solar radiation, as can be confirmed in Figures 17 and 18. In this case, both battery voltage and current fluctuations have been significantly reduced, either in steady state or in the case of a pulsating load that has been assigned to the SCs, which reveals that the battery dynamic stress level is reduced and hence battery lifespan could be prolonged. Furthermore, as the MPPT is increased under the pulsating load (from 1.4 s to 1.6 s) with low-solar radiation, as previously mentioned, the power supplied by the battery is decreased accordingly, as shown in Figure 19. In addition, the battery state of charge is improved in case of utilizing the SC with the battery storage unit, as shown in Figure 20, which dedicates a saved energy and could increase the system efficiency. Figures 21 and 22 show the performance of the SC during the implementation of the proposed EMS control technique. As expected, the SC voltage and current are highly pulsating to compensate the fluctuations in different system buses: PV, load, and battery voltages and currents.

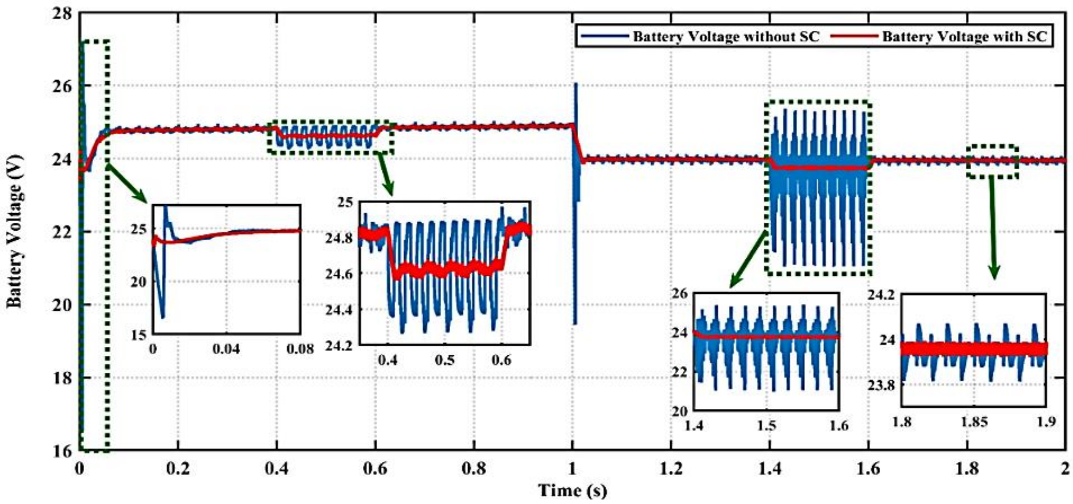


Figure 17. Simulated battery voltage waveforms

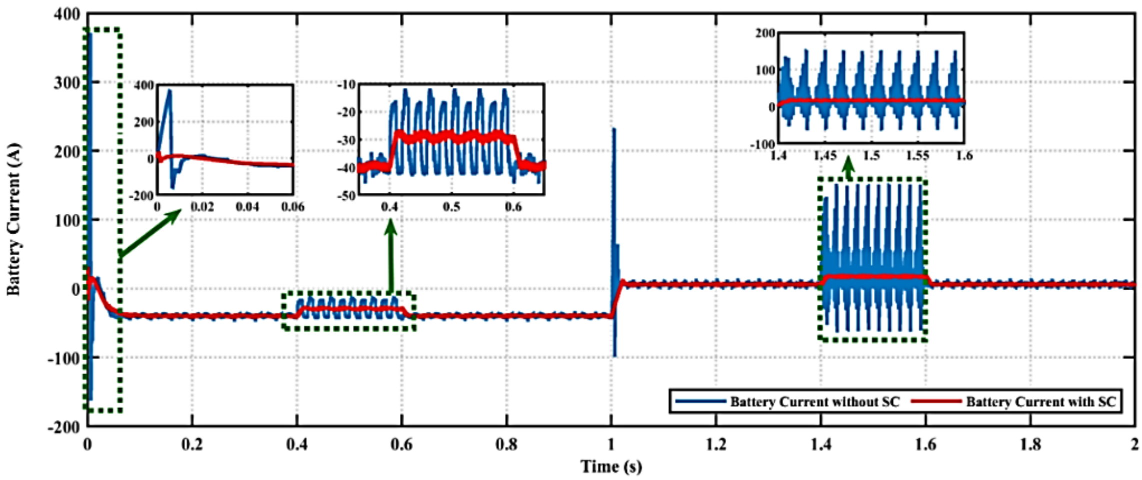


Figure 18. Simulated battery current waveforms

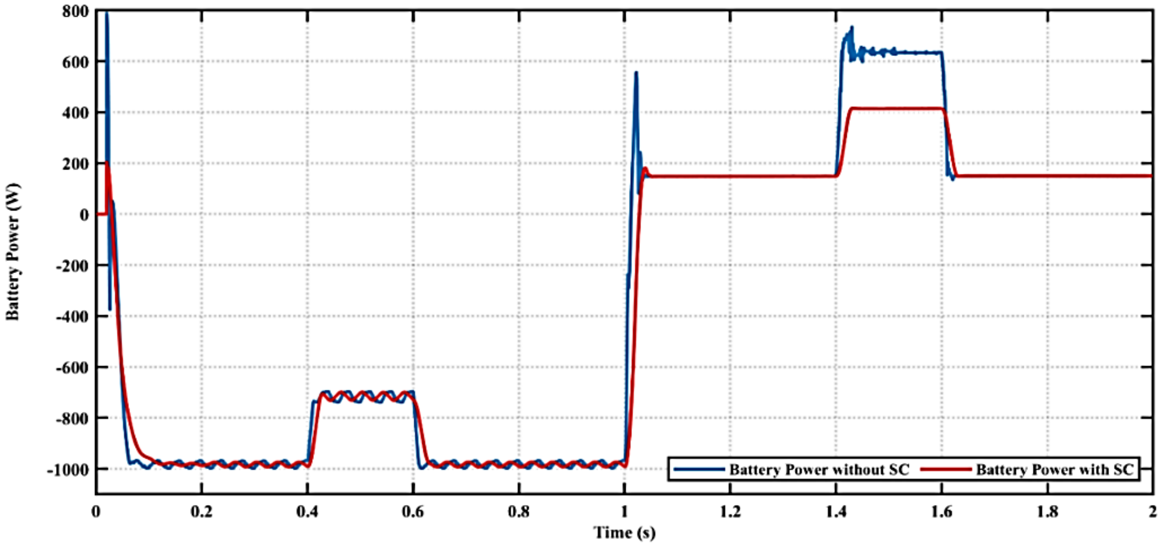


Figure 19. Simulated battery power waveforms

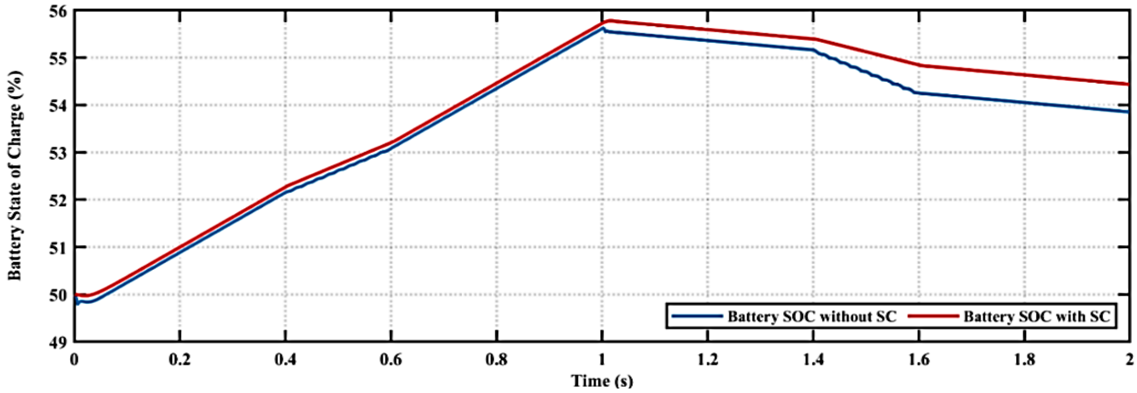


Figure 20. Battery state of charge waveform

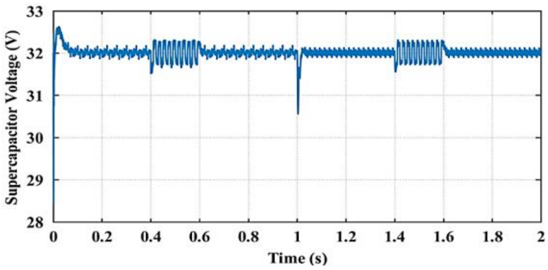


Figure 21. Supercapacitor terminal voltage waveform

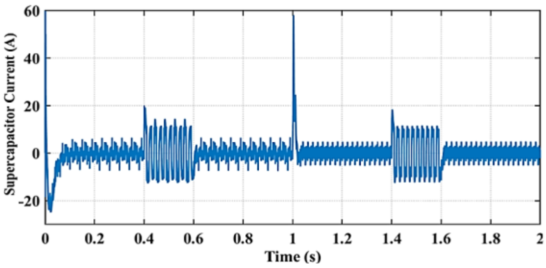


Figure 22. Supercapacitor current waveform

Figure 23 presents a comparative generated/absorbed power for the different system units: PV, battery, load, and SC. From this figure, it becomes clear that the adoption of the SC with the suggested EMS control technique improved the MPPT performance and increased the MPP mechanism, which is reflected as saved energy in the battery at the low-solar radiation region. Moreover, at the starting instant, the PV power with SC included tracks the MPP faster than the PV power without the SC storage unit. Additionally, in low-solar radiation, the PV power with SC included (red-colored waveform) secures a constant MPPT value compared to a reduced generated power in the absence of SC (cerulean-colored waveform). It is paramount to mention that the average power of SC (black-colored waveform) is zero in steady-state condition, whereas its value changed during the transient states of charging/discharging to compensate the battery power (violetcolored waveform), resulting in a smoothed battery power with SC storage unit (green-colored waveform) as a HEES system.

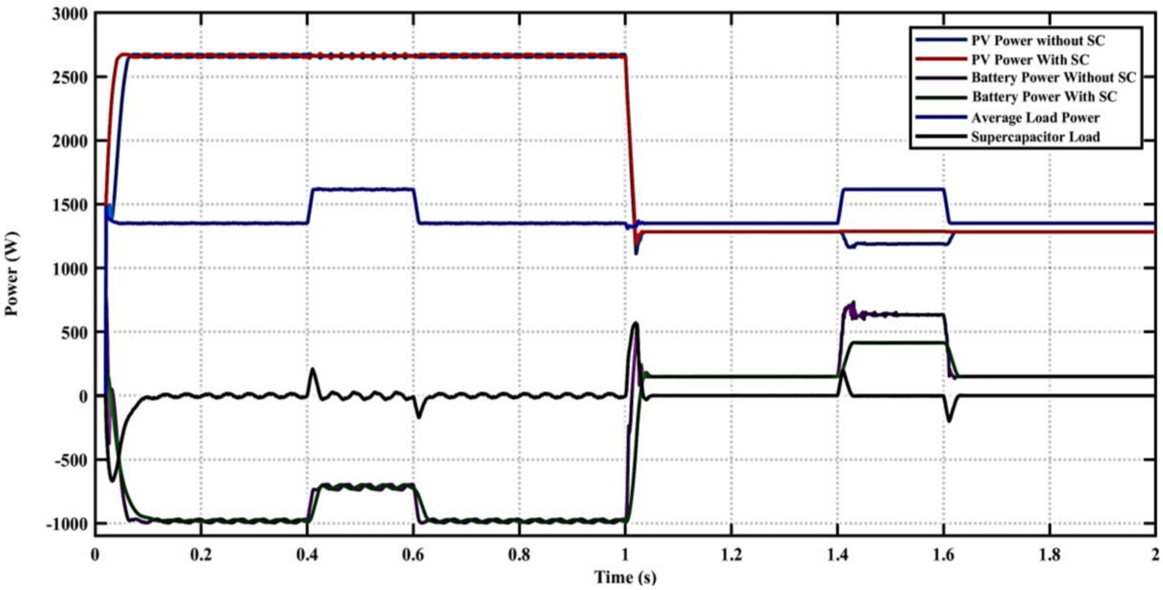


Figure 23. Simulated power waveforms of different system units under variation in solar radiation and load

## 6. CONCLUSION

The effect of using SCs with a proposed EMS approach is investigated in this study to improve the performance of a PV system and battery in a standalone hybrid system while feeding a pulsating load in addition to a base load demand. System modeling and sizing have been introduced, and then an EMS control strategy has been proposed. The merits achieved by utilizing the SC storage unit in conjunction with battery with the proposed EMS approach include fast dynamic response, and reduced load terminal voltage and current ripples, smoothed battery current and voltage, decreased PV voltage and current fluctuations, and finally enhanced the MPPT mechanism either in high- or low-solar radiation. Consequently, several outcomes arise: reduced battery dynamic stress level and hence increased battery lifetime, saved battery power and hence a more efficient system, and improved overall system dynamic performance. As a future direction of the current research study, the recent optimization techniques could be used to achieve further improvement in the dynamic performance HEES system for the standalone PV system feeding pulsating loads.

## ACKNOWLEDGEMENTS

This work was financially supported by scientists for next generation (SNG) program, Academy of Scientific Research and Technology, Ministry of Higher Education & Scientific Research, Cairo, Egypt.

## REFERENCES

[1] M. G. Villalva, J. R. Gazoli, and E. R. Filho, “Comprehensive Approach to Modeling and Simulation of Photovoltaic Arrays,” *IEEE Transactions on Power Electronics*, vol. 24, no. 5, pp. 1198–1208, May 2009, doi: 10.1109/TPEL.2009.2013862.

[2] M. E. Glavin, P. K. W. Chan, and W. G. Hurley, “Optimization of autonomous hybrid energy storage system for photovoltaic applications,” *2009 IEEE Energy Conversion Congress and Exposition, ECCE 2009*, pp. 1417–1424, 2009, doi: 10.1109/ECCE.2009.5316370.

[3] P. T. Moseley, “Energy storage in remote area power supply (RAPS) systems,” *Journal of Power Sources*, vol. 155, no. 1, pp. 83–87, 2006, doi: 10.1016/j.jpowsour.2004.10.036.

[4] H. Guentri, T. Allaoui, M. Mekki, and M. Denai, “POWER management and control of A PHOTOVOLTAIC system with hybrid battery-supercapacitor energy storage Based On Heuristics Methods,” *Journal of Energy Storage*, vol. 39, 2021, doi: 10.1016/j.est.2021.102578.

[5] R. Sathishkumar, S. K. Kollimalla, and M. K. Mishra, “Dynamic energy management of micro grids using battery super capacitor combined storage,” *2012 Annual IEEE India Conference, INDICON 2012*, pp. 1078–1083, 2012, doi: 10.1109/INDCON.2012.6420777.

[6] M. E. Glavin, P. K. W. Chan, S. Armstrong, and W. G. Hurley, “A stand-alone photovoltaic supercapacitor battery hybrid energy storage system,” *2008 13th International Power Electronics and Motion Control Conference, EPE-PEMC 2008*, pp. 1688–1695, 2008, doi: 10.1109/EPEPEMC.2008.4635510.

[7] Y. Kim, V. Raghunathan, and A. Raghunathan, “Design and Management of Battery-Supercapacitor Hybrid Electrical Energy

Storage Systems for Regulation Services," *IEEE Transactions on Multi-Scale Computing Systems*, vol. 3, no. 1, pp. 12–24, 2017, doi: 10.1109/TMSCS.2016.2627543.

[8] W. L. Jing, C. H. Lai, W. S. H. Wong, and M. L. Dennis Wong, "Cost analysis of battery-supercapacitor hybrid energy storage system for standalone pv systems," *IET Conference Publications*, vol. 2016, no. CP688, 2016, doi: 10.1049/cp.2016.1288.

[9] W. Jing, C. H. Lai, D. K. X. Ling, W. S. H. Wong, and M. L. D. Wong, "Battery lifetime enhancement via smart hybrid energy storage plug-in module in standalone photovoltaic power system," *Journal of Energy Storage*, vol. 21, pp. 586–598, 2019, doi: 10.1016/j.est.2018.12.007.

[10] T. Ma, H. Yang, and L. Lu, "Development of hybrid battery-supercapacitor energy storage for remote area renewable energy systems," *Applied Energy*, vol. 153, pp. 56–62, 2015, doi: 10.1016/j.apenergy.2014.12.008.

[11] W. Jing, C. H. Lai, W. S. H. Wong, and M. L. D. Wong, "A comprehensive study of battery-supercapacitor hybrid energy storage system for standalone PV power system in rural electrification," *Applied Energy*, vol. 224, pp. 340–356, 2018, doi: 10.1016/j.apenergy.2018.04.106.

[12] Y. Wang, L. Wang, M. Li, and Z. Chen, "A review of key issues for control and management in battery and ultra-capacitor hybrid energy storage systems," *eTransportation*, vol. 4, 2020, doi: 10.1016/j.etran.2020.100064.

[13] Q. Zhang, L. Wang, G. Li, and Y. Liu, "A real-time energy management control strategy for battery and supercapacitor hybrid energy storage systems of pure electric vehicles," *Journal of Energy Storage*, vol. 31, 2020, doi: 10.1016/j.est.2020.101721.

[14] L. W. Chong, Y. W. Wong, R. K. Rajkumar, and D. Isa, "Modelling and Simulation of Standalone PV Systems with Battery-supercapacitor Hybrid Energy Storage System for a Rural Household," *Energy Procedia*, vol. 107, pp. 232–236, 2017, doi: 10.1016/j.egypro.2016.12.135.

[15] Q. Zhang and G. Li, "Experimental study on a semi-active battery-supercapacitor hybrid energy storage system for electric vehicle application," *IEEE Transactions on Power Electronics*, vol. 35, no. 1, pp. 1014–1021, 2020, doi: 10.1109/TPEL.2019.2912425.

[16] L. W. Chong, Y. W. Wong, R. K. Rajkumar, and D. Isa, "An optimal control strategy for standalone PV system with Battery-Supercapacitor Hybrid Energy Storage System," *Journal of Power Sources*, vol. 331, pp. 553–565, 2016, doi: 10.1016/j.jpowsour.2016.09.061.

[17] L. Kouchachvili, W. Yaïci, and E. Entchev, "Hybrid battery/supercapacitor energy storage system for the electric vehicles," *Journal of Power Sources*, vol. 374, pp. 237–248, 2018, doi: 10.1016/j.jpowsour.2017.11.040.

[18] R. Xiong, H. Chen, C. Wang, and F. Sun, "Towards a smarter hybrid energy storage system based on battery and ultracapacitor - A critical review on topology and energy management," *Journal of Cleaner Production*, vol. 202, pp. 1228–1240, 2018, doi: 10.1016/j.jclepro.2018.08.134.

[19] D. Lemian and F. Bode, "Battery-Supercapacitor Energy Storage Systems for Electrical Vehicles: A Review," *Energies*, vol. 15, no. 15, 2022, doi: 10.3390/en15155683.

[20] N. Pandiarajan and R. Muthu, "Mathematical modeling of photovoltaic module with Simulink," in *2011 1st International Conference on Electrical Energy Systems*, IEEE, Jan. 2011, pp. 258–263. doi: 10.1109/ICEES.2011.5725339.

[21] O. Tremblay, L.-A. Dessaint, and A.-I. Dekkiche, "A Generic Battery Model for the Dynamic Simulation of Hybrid Electric Vehicles," in *2007 IEEE Vehicle Power and Propulsion Conference*, IEEE, Sep. 2007, pp. 284–289. doi: 10.1109/VPPC.2007.4544139.

[22] M. R. M. Hassan, M. A. Mossa, and G. M. Dousoky, "Evaluation of electric dynamic performance of an electric vehicle system using different control techniques," *Electronics (Switzerland)*, vol. 10, no. 21, 2021, doi: 10.3390/electronics10212586.

[23] R. L. Spyker and R. M. Nelms, "Classical equivalent circuit parameters for a double-layer capacitor," *IEEE Transactions on Aerospace and Electronic Systems*, vol. 36, no. 3, pp. 829–836, Jul. 2000, doi: 10.1109/7.869502.

[24] S. Njoya Motapon, L. A. Dessaint, and K. Al-Haddad, "A comparative study of energy management schemes for a fuel-cell hybrid emergency power system of more-electric aircraft," *IEEE Transactions on Industrial Electronics*, vol. 61, no. 3, pp. 1320–1334, 2014, doi: 10.1109/TIE.2013.2257152.

[25] H. Miniguano, A. Barrado, C. Fernández, P. Zumel, and A. Lázaro, "A general parameter identification procedure used for the comparative study of supercapacitors models," *Energies*, vol. 12, no. 9, 2019, doi: 10.3390/en12091776.

[26] V. G. R. Kummara *et al.*, "A comprehensive review of DC–DC converter topologies and modulation strategies with recent advances in solar photovoltaic systems," *Electronics (Switzerland)*, vol. 9, no. 1, 2020, doi: 10.3390/electronics9010031.

[27] A. Kuperman and I. Aharon, "Battery-ultracapacitor hybrids for pulsed current loads: A review," *Renewable and Sustainable Energy Reviews*, vol. 15, no. 2, pp. 981–992, 2011, doi: 10.1016/j.rser.2010.11.010.

## BIOGRAPHIES OF AUTHORS

**Mohamed Salah Hassan** received the B.Sc. and M.Sc. degrees in Electrical Engineering from Minia University, Minia, Egypt, in 2010 and 2016, respectively, and the Ph.D. degree with a focus on power electronics from Kyushu University, Fukuoka, Japan, in 2020. Since 2011, he has been a member of the Faculty of Engineering, Minia University. In 2017, he was awarded a full Ph.D. scholarship from the partnership on education: Egypt-Japan Education Partnership (EJEP). Moreover, he received several travel grants from different foundations such as Power Sources Manufacturers Association (PSMA), USA, Telecommunications Advancement Foundation, and Kyudai Foundation, Japan, to support attending international conferences. He was the recipient of the Annual Best Master's thesis from Minia University in 2016 and the 2019 Excellent Student Award of the IEEE Fukuoka Section. He is currently a postdoctoral research fellow at Kyushu University. His research interests include high-frequency DC/AC pulse width modulated inverters for renewable energy sources, electromagnetic interference/compatibility (EMI/EMC), energy management systems (EMS), and cryogenic power electronics. He can be contacted at email: m.salah@mu.edu.eg.

**Shimaa Hassan** is a master student in the Electrical Engineering Department, Minia University, Egypt. She received the B.Sc. degree in Electrical Engineering from Minia University, Egypt, in 2016. Her research interests include the field of renewable energy, power electronics, industrial applications, photovoltaic power systems, and energy management system. She can be contacted at email: shimaahassan201092@gmail.com.

**Mohamed Reda Mahmoud Hassan** is an assistant lecturer in Electrical and Electronic Engineering Department, Mini University, Egypt since February 2023; and he has been a demonstrator since January 2019. He received the B.Sc. and M.Sc. degrees in electrical and electronic engineering from Minia University, Egypt, in 2018 and 2023, respectively. His research interests include the field of power electronics, motor drives, industrial applications, industrial electronics, photovoltaic power systems, digital control, electric vehicles, and energy management systems. He can be contacted at email: mohamed.hassan@mu.edu.eg.

**Abou-Hashema Mostafa El-Sayed** received his B.Sc., and M.Sc. in Electrical Engineering from Minia University, Minia, Egypt, in 1994 and 1998, respectively. He was a Ph.D. student in the Institute of Electrical Power Systems and Protection, Faculty of Electrical Engineering, Dresden University of Technology, Dresden, Germany from 2000 to 2002. He received his Ph.D. in Electrical Power from the Faculty of Engineering, Minia University, Egypt in 2002, according to a channel system program, which means a Scientific Co-operation between the Dresden University of Technology, Germany and Minia University, Egypt. Since 1994, he has been with the Electrical Engineering Department, Faculty of Engineering, Minia University, as a Teaching Assistant, a Lecturer Assistant, an Assistant Professor, Associate Professor and A full professor. He was a Visiting Researcher at Kyushu University, Japan, from 2008 to 2009. He is the head of Mechatronics and Industrial Robotics Program, Faculty of Engineering, Minia University from 2011 till now. His research interests include Protection systems, renewable energy, and power systems. He can be contacted at email: abouhashema@mu.edu.eg.

**Masahito Shoyama** received the B.S. degree in electrical engineering and the Dr. Eng. from Kyushu University, Fukuoka, Japan, in 1981 and 1986, respectively. In 1986, he joined as a Research Associate with the Department of Electronics, Kyushu University, where he has been an Associate Professor since 1990, and a professor since 2010. Since 2009, he has been with the Department of Electrical Engineering, Faculty of Information Science and Electrical Engineering, Kyushu University. His research interests include the field of power electronics, especially in the areas of bidirectional converters for DC/AC power systems, high frequency switching converters for renewable energy sources, power factor correction (PFC) converters, and electromagnetic compatibility (EMC). Prof. Shoyama is a member of the Institute of Electronics, Information and Communication Engineers (IEICE), Institute of Electrical Engineers of Japan (IEEJ), and Society of Instrument and Control Engineers (SICE). He can be contacted at email: shoyama@ees.kyushu-u.ac.jp.

**Gamal Mahmoud Dousoky** received the B.Sc. and M.Sc. degrees in electrical and electronic engineering from Minia University, Egypt, in 2000 and 2004, respectively, and the Ph.D. degree in electrical and electronic engineering from Kyushu University, Japan, in 2010. Since 2000, he has been associated with the Department of Electrical Engineering, Faculty of Engineering, Minia University. In March 2022, he was promoted to the position of a professor position. He authored and coauthored more than 90 publications, in international journals and conference proceedings of Power Electronics and Industrial Technologies. His research interests include power electronics, particularly renewable energy applications, energy efficiency, switching power supplies, electromagnetic interference/compatibility, and digital control. Prof. Dousoky received the 2009 Excellent Student Award of the IEEE Fukuoka Section. He is also a reviewer in many international journals and conferences. He can be contacted at email: dousoky@mu.edu.eg.